

1.2 Characterization of Churn-Turbulent Bubble Columns

The scaleup equations for gas holdup and liquid recirculating velocity presented in the 12th quarterly report and the equations for turbulent eddy diffusivities presented above have been developed for air-water atmospheric systems in the churn-turbulent regime. In this flow regime, the effects of the gas distributor and trace contaminants in water are expected to be small. It is therefore assumed that at sufficiently high gas velocities for air-water systems, the fluid dynamic parameters are predominantly a function of superficial gas velocity and column diameter.

A change in system properties (e.g., physical properties of the fluids, presence of solids) and operating conditions (pressure and temperature) directly affects bubble sizes and their distribution, and thereby the global gas holdup and holdup distribution in the column. This in turn influences the extent of liquid recirculation and turbulence characteristics in the system, which are essentially dictated by the passage and interaction of bubbles. For example, an increase in the system pressure tends to reduce the bubble size, which delays transition to turbulent flow regime, and therefore results in the increase in gas holdup, compared to values expected at atmospheric conditions. However, when the flow is in the churn-turbulent regime, it is typically characterized by the presence of large and small bubbles, irrespective of system pressure and other such factors (Krishna and Ellenberger, 1996; De Swart, 1996). Based on interpretation of dynamic gas disengagement (DGD) experiments, Krishna et al. (1994) conclude that the characteristics of the large bubbles are unaffected by system properties and pressure. Independent measurements of the local holdup profile in high-pressure bubble columns, at high gas velocities (Adkins et al., 1996), indicate that the holdup profile is parabolic ($m = 2$ in Equation 1.7), similar to the case for air-water systems at atmospheric pressure.

$$\varepsilon_g = \tilde{\varepsilon}_g \frac{m+2}{m} (1 - c\xi^m) \quad (1.7)$$

From these observations it is inferred that well into the churn-turbulent flow regime, similar bimodal bubble size distribution is present in the column, irrespective of system properties (except when viscosity is very high). It is essentially the resulting gas holdup and its radial distribution that dictate liquid recirculation and turbulence. Therefore, the unified characterization of churn-turbulent bubble columns can be employed to approximately evaluate \bar{u}_{rec} , \bar{D}_{zz} and \bar{D}_{rr} in industrial systems of interest, based on the knowledge of these parameters in air-water systems, as shown in Figure 1.5. For a given process condition, with prior knowledge of the global gas holdup in the column, an equivalent superficial gas velocity, U_{ge} , which would exist at atmospheric conditions in such a column in an air-water system, can be evaluated using Equation 1.8.

$$\bar{\varepsilon}_g = 0.07U_g^{0.474-0.000626D_c} \quad (\text{in cgs units}) \quad (1.8)$$

The calculated U_{ge} can then be substituted in Equations 1.1 to 1.4, as well as Equation 1.9, to estimate the average turbulent diffusivities and average recirculation rate in the column under the specific conditions of interest.

$$\bar{u}_{rec} (cm/s) = 2.2 D_c^{0.4} U_g^{0.4} \quad (1.9)$$

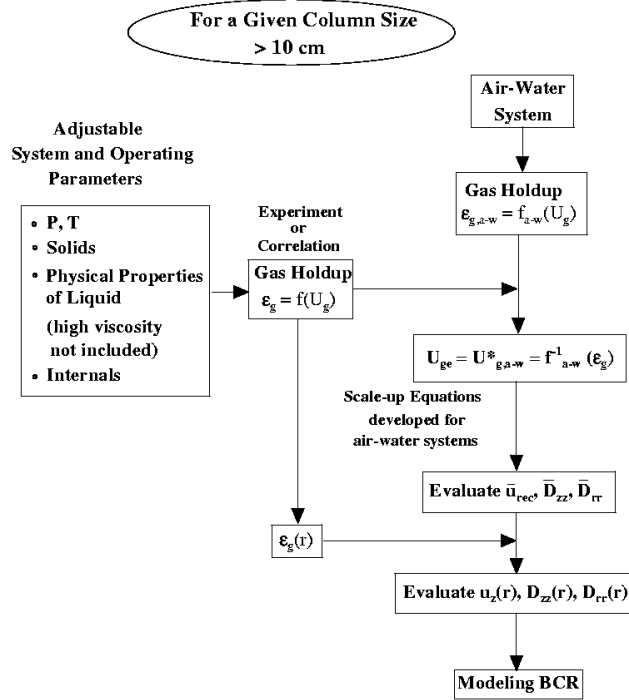


Figure 1.5 Method of Characterization of Churn-Turbulent Bubble Columns

The fluid dynamic parameters estimated from the above procedure are used in the phenomenological modeling of liquid mixing in an industrial slurry bubble column reactor, namely the AFDU in LaPorte, Texas.

1.3 Summary

Using experimental data obtained by CARPT/CT and from the literature, equations have been developed to predict the mean liquid recirculating velocity and average eddy diffusivities in air-water atmospheric systems. Based on the unified characterization of churn-turbulent bubble columns, a methodology has been proposed which enables the estimation of the mean liquid recirculating velocity and turbulent eddy diffusivities, in churn-turbulent flow regime, in systems of industrial interest (e.g., high pressure and high temperature), using the data generated in air-water systems. This strategy requires a knowledge of the global holdup and holdup distribution in the system under consideration.

The equations and proposed methodology for the scaleup of churn-turbulent bubble columns require substantiation with additional experimental data for the fluid dynamic parameters in large columns, at higher gas velocities and in different systems. Once verified, these will serve as tools by which data from a limited database can be utilized to model and scale up bubble columns, under process conditions, in the churn-turbulent flow regime. The following section

discusses an indirect verification of the scaleup strategy, which was accomplished by interpreting the experimental liquid tracer data obtained in the LaPorte ADFU.

1.4 References

Adkins, D. R., K. A. Shollenberger, T. J. O'Hern, and J. R. Torczynski, "Pressure Effects on Bubble Column Flow Characteristics," *ANS Proceedings of the National Heat Transfer Conference*, THD-Vol. 9, 318-325 (1996).

De Swart, J. W. A., "Scaleup of a Fischer-Tropsch Slurry Reactor," Ph.D. Thesis, University of Amsterdam, The Netherlands (1996).

Degaleesan, S., "Fluid Dynamic Measurements and Modeling of Liquid Mixing in Bubble Columns," D.Sc. Thesis, Washington University, St. Louis, MO (1997).

Krishna, R., and J. Ellenberger, "Gas Holdup in Bubble Column Reactors Operating in the Churn-Turbulent Flow Regime," *AIChE J.*, Vol. 42, 2627-2634 (1996).

Krishna, R., J. W. A. de Swart, D. E. Hennephof, J. Ellenberger, and H. C. J. Hoefsloot, "Influence of Increased Gas Density on Hydrodynamics of Bubble Column Reactors," *AIChE J.*, Vol. 40, 112-119 (1994).

2. Interpretation of the Liquid Phase Tracer Data during Methanol Synthesis at the LaPorte AFDU using the Fundamental Two-Dimensional Convection-Diffusion Model

A two-dimensional convection-diffusion model for liquid mixing in bubble columns has been developed to interpret the liquid phase tracer data taken at the LaPorte AFDU during methanol synthesis. The model equations were reported in the seventh quarterly report. The model characterizes, in a statistical sense, the large-scale flow pattern and mixing in the column, which should prove useful for the design and scaleup of bubble column reactors.

It is noted that, since long time averaging is used to arrive at the model equations, the current model only describes the meso- and macro-scale mixing in the column. Micromixing phenomena are not captured, but this is not a serious drawback since most of the reactions in bubble columns are slow to moderately fast, and the characteristic reaction time is longer than the micromixing time scale.

In this section, the two-dimensional convection-diffusion model developed is used to interpret the liquid phase tracer runs performed during methanol synthesis at the LaPorte AFDU. The model parameters obtained were based on the developed scaleup methodology from CARPT measurements using as input the estimated radial gas holdup profile at LaPorte, which was estimated from the Nuclear Gauge Densitometry and pressure drop measurements. The developed scaleup procedure for the gas holdup and liquid recirculating velocity was reported in

the previous quarterly report (12th quarter), while the turbulent eddy diffusivities are provided in Section 1 of this report.

Although the developed model was described in the seventh quarterly report, we re-state it here for clarity and for ease in following its implementation.

2.1 Two-Dimensional Convection-Diffusion Model for Liquid Mixing in Bubble Columns

The fundamental two-fluid model mass balance equation for the local, instantaneous tracer species for phase k is given by the following equation:

$$\frac{\partial \rho_k C_k}{\partial t} + \nabla \cdot \rho_k C_k \bar{u}_k - D_m \nabla^2 C_k = 0 \quad (2.1)$$

with an interfacial jump condition for mass transfer across the interface:

$$\sum_{k=1}^2 \rho_k C_k [\bar{u}_k - \bar{u}_{ki}] \cdot \bar{n}_k = 0 \quad (2.2)$$

In the equation above, the phase density, ρ_k , for incompressible flows such as those in bubble columns, can be considered to be constant. D_m is the molecular diffusivity, which is small and will be ignored hereafter. Phasic or ensemble averaging of the above equation in an axisymmetric system for an inert, non-volatile tracer yields:

$$\begin{aligned} & \frac{\partial}{\partial t} \left(\rho_k \varepsilon_k \langle C_k \rangle^x \right) + \frac{\partial}{\partial z} \rho_k \left(\varepsilon_k \langle u_{z,k} \rangle^x \langle C_k \rangle^x + \varepsilon_k \langle u'_{z,k} C_k' \rangle^x \right) + \\ & \frac{1}{r} \frac{\partial}{\partial r} r \rho_k \left(\varepsilon_k \langle u_{z,k} \rangle^x \langle C_k \rangle^x + \varepsilon_k \langle u'_{z,k} C_k' \rangle^x \right) = \langle \rho_k C_k (\bar{u}_k - \bar{u}_{ki}) \cdot \nabla X_k \rangle \end{aligned} \quad (2.3)$$

where $\langle \rangle^x$ represents phasic averaging. The right-hand side of Equation 2.3 represents the term due to mass transfer across the interface, where X_k is the phase function and is defined as in Equation 2.4.

$$X_k(\bar{x}, t) = \begin{cases} 1 & \text{if } \bar{x} \text{ is in phase } k \text{ at time } t \\ 0 & \text{otherwise} \end{cases} \quad (2.4)$$

An additional source term to represent reaction can be added to the right-hand side of the equation. For the current situation, considering a non-volatile inert liquid tracer, the right-hand side of Equation 2.3 is set to 0. Since the model is primarily concerned with the liquid phase, the subscript $k = l$, denoting the liquid phase, is dropped. In addition, all symbols denoting averaging are dropped in order to simplify notation. All the variables representing the fluid dynamic parameters and the tracer concentration will denote the phase-averaged quantities.

The cross-correlation terms between the fluctuating velocity and tracer concentration are closed using a standard gradient diffusion model (Hinze, 1975; Tennekes and Lumley, 1971; Seinfeld, 1986), as

$$\langle u'_z C' \rangle^x = -D_{zr} \frac{\partial C}{\partial r} - D_{zz} \frac{\partial C}{\partial z} \quad (2.5)$$

and

$$\langle u'_r C' \rangle^x = -D_{rr} \frac{\partial C}{\partial r} - D_{rz} \frac{\partial C}{\partial z} \quad (2.6)$$

but, CARPT experiments show that

$$D_{zr} = D_{rz} \sim 0 \quad (2.7)$$

Therefore

$$\langle u'_z C' \rangle^x = -D_{zz} \frac{\partial C}{\partial z} \quad (2.8)$$

$$\langle u'_r C' \rangle^x = -D_{rr} \frac{\partial C}{\partial r} \quad (2.9)$$

where D_{zz} and D_{rr} are the CARPT measured axial and radial turbulent eddy diffusivities, respectively. Therefore, the final form of the model equation is:

$$\frac{\partial(\varepsilon C)}{\partial t} + \frac{\partial}{\partial z}(\varepsilon u_z C) + \frac{1}{r} \frac{\partial}{\partial r}(r \varepsilon u_r C) = \frac{1}{r} \frac{\partial}{\partial r}[r \varepsilon D_{rr} \frac{\partial C}{\partial r}] + \frac{\partial}{\partial z}[\varepsilon D_{zz} \frac{\partial C}{\partial z}] \quad (2.10)$$

Standard boundary conditions are used with zero flux at the wall and at the centerline of the column. For the case with continuous flow of liquid through the column, a zero gradient is assumed at the outlet, with injection of tracer at the inlet. Equation 2.10 represents the averaged balance equation for the non-volatile liquid species, and is a transient, two-dimensional convection-diffusion equation. The phasic (or time) averaging refers to any time interval, which may be small or large.

Multiphase flows in bubble columns are highly transient in nature. Hence the length of the time interval considered in the averaging will affect the type of results obtained. Short time averages involve averaging conducted over a short time interval, long enough to smooth the variations across the interface, but short enough to capture some of the transient structures in the flow. These transient structures will vary in nature with the time interval of averaging. On the other hand, long time averaging results in a statistically stationary flow field, which is steady in time, in terms of all the fluid dynamic variables.

Two factors are of concern here in deciding the type of averaging to be considered for the above model equation. First, since the flow phenomena in bubble columns are highly turbulent and random in nature, a quantitative comparison of the fluid dynamic parameters, between model predictions and experimental measurements, can be made only with respect to the statistical properties of the flow field. This immediately implies that time or ensemble averaging is required. Second, since the current model is considered in a two-dimensional axisymmetric domain, the type of boundary conditions used (zero gradient at the centerline) will not permit the computation of physically realistic results describing the transient structures. A true transient

behavior can only be represented in a fully three-dimensional flow model, which can capture the inherent vortical and spiraling motion of the flow in bubble columns.

For these reasons, we propose to consider long time averaging for the above model equation. The various averaged quantities in the above equation will hence refer to long time-averaged quantities and corresponding closure models (Equations 2.8 and 2.9). CARPT data for the long time-averaged liquid velocities, u_r and u_z , and turbulent diffusivities, D_{rr} and D_{zz} , along with CT data for the time-averaged liquid holdup profile, are used as input parameters to the model.

2.2 Numerical Procedure for Solution of Model Equations

A finite volume (also referred to as the control volume) method has been used to solve the convection-diffusion model (Patankar, 1983). In this scheme, the calculation domain is divided into a number of non-overlapping control volumes, such that there is a control volume surrounding each grid point. The governing equations are integrated over each volume, with piece-wise profiles for the variation in the dependent variables. This results in the discretization equation containing the values of the dependent variables for a group of grid points. The discretization equation obtained as such allows the conservation principle for a given quantity to be expressed for the finite control volume. The most attractive aspect of this method is that the resulting solution guarantees that the integral conservation of a given quantity is exactly satisfied over a single or group of control volumes, and therefore over the whole domain. Thus, even the coarse-grid solution exhibits exact integral balances.

2.2.1 Discretization Considerations

An implicit scheme is used in time, with upwinding for the convection term. Although the upwind scheme is only first-order accurate, it has been shown to have advantages in solving nonlinear systems with steep velocity gradients (Patankar, 1980), as in the case of bubble column flows. However, if the physical diffusion process is dominant (i.e., if D_{zz} and D_{rr} are very large), upwind differencing loses its advantages and requires finer discretization. A staggered grid configuration is used by assigning the scalar variables, namely the concentration and holdup to the cell center and the vector velocity variables and diffusivities to the cell faces (Figure 2.1). Advantages of using the staggered grid configuration, for solution of the momentum balance equations, have been discussed elaborately by Verstaag et al. (1995) and Patankar (1983). For solution of the convection-diffusion equation it poses no special advantage.

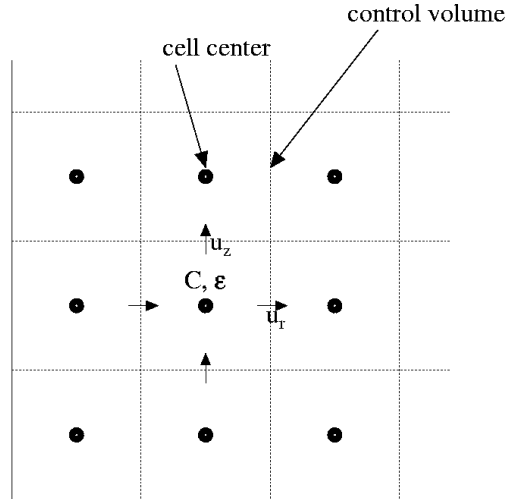


Figure 2.1 Variable Locations in a Staggered Grid

The above process of discretization results in a set of linear algebraic equations. Since the model equation is a transient convection-diffusion equation, this results in a sparse matrix. Therefore a direct method is used to solve the system of equations, based on LU decomposition. The model is two dimensional, resulting in extremely large number of equations that depend on the size of the domain studied. The SMPAKTM solver, which uses an effective storage scheme to hold large sparse matrices, is used to solve the equations. This significantly reduces the memory and time (five times less than a standard solver) for computation. The spacing used in the three coordinates, Δt , Δz and Δr , are the numerical parameters that need to be considered. Although stability is not a concern since an implicit scheme is used, the issue of accuracy should be examined. For this purpose, several trials are made with increasingly fine discretizations, until an accurate solution is obtained.

There is considerable experimental evidence in the literature, including results from CARPT, which show that in columns of high aspect ratios, the time-averaged flow pattern is axisymmetric, with global liquid recirculation in the column. In a time-averaged sense, a large-scale liquid circulation exists in the form of a recirculation cell, which occupies most of the column with respect to height, with liquid ascending along the central core region and descending along the annular region between the core and the walls. A single one-dimensional velocity profile is always identified in this recirculation cell, which is in the middle part of the column. Axial variations are evident in the distributor and free surface region, where the liquid turns around. In the middle region, there is evidence that all the other fluid dynamic parameters, such as the turbulent eddy diffusivities and the turbulent stresses, are also a function of radial position only.

The computation domain is therefore divided axially into three regions: a distributor zone at the bottom, a fully developed region where the radial liquid velocities are negligible and are considered to be zero, and finally the disengagement zone at the top where liquid turns around. The distributor and disengagement zones are assumed to extend over a height equal to one

column diameter, based on experimental considerations. However, varying the height from 1 to 2 times the column diameter does not affect the results significantly (Figure 2.6), especially for column aspect ratios greater than 10. In the distributor zone and the disengagement zone, the domain is discretized only in the radial direction, as shown in Figure 2.2. In both these regions where the radial liquid velocities are significant, the solution of the equations becomes very sensitive to the radial velocities. The velocities assigned to these regions are therefore fitted to a smooth profile in order to satisfy liquid continuity for each control volume or cell, and therefore the entire domain. In the fully developed middle region, the domain is discretized both radially and axially (Figure 2.2), and the radial liquid velocities are set to zero.

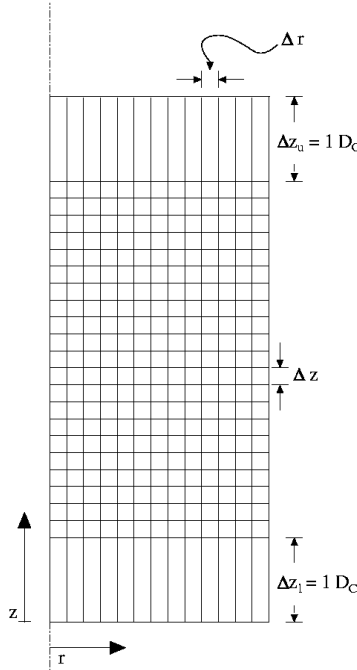


Figure 2.2 Schematic of Column Discretization

The other fluid dynamic variables, i.e., the axial liquid velocity, axial and radial turbulent eddy diffusivities, are considered to be a function of radial position only, and independent of axial location in the middle section of the column. Experimental data from CT for the gas holdup is first fitted to the power law expression given by Equation 2.11 to obtain the radial liquid holdup profile. This profile is then used as an input to the one-dimensional liquid recirculation model to obtain an axial liquid velocity profile that fits the experimental data from CARPT measurements under the same operating conditions.

$$\varepsilon_g = \tilde{\varepsilon}_g \frac{m+2}{m} (1 - c\xi^m) \quad , \quad \varepsilon_l = 1 - \varepsilon_g \quad (2.11)$$

These radial profiles for the liquid holdup and velocity are used as input to the model in the middle, fully developed section of the column, along with radial profiles for the axial and radial turbulent eddy diffusivities. Using these calculated profiles for the holdup and velocity ensures

that continuity is satisfied in the entire domain. The developed model, as represented by Equation 2.10, is used to simulate tracer responses for different cases for which experimental data are available.

2.3 Case I: Air-Water System

The model is first tested in a column under operating conditions for which experimental data for the fluid dynamic parameters are directly available. The case considered is the tracer data of Myers et al. (1986), whose experiments were conducted in an air-water system in a 19-cm diameter column, at a superficial gas velocity of 10 cm/s and liquid velocity of 1 cm/s. The mode of operation, in this case, is therefore a cocurrent bubble column with a continuous flow of liquid and gas. The following boundary conditions are used:

$$r = 0, \text{ and } r = R; \quad \frac{\partial C}{\partial r} = 0 \quad (2.12 \text{ a, b})$$

$$z = 0, C(r,0,t) = \delta(t); \quad z = L, \quad \frac{\partial C}{\partial z} = 0 \quad (2.12 \text{ c, d})$$

$$t = 0, C(r,z,0) = 0 \quad (2.13)$$

A time step of 0.5 sec along with a radial grid size of 0.38 cm and an axial grid size of 1 cm were found to be optimum discretizations. In the end zones, the cell heights were assigned to be equal to the column diameter. In order to solve the model for the present case, CARPT and CT experiments were performed under identical conditions to obtain the input hydrodynamic parameters for the system. Results are shown in Figures 2.3, 2.4 and 2.5 for the one-dimensional, time-averaged axial liquid velocity, liquid holdup profile and turbulent eddy diffusivities, respectively.

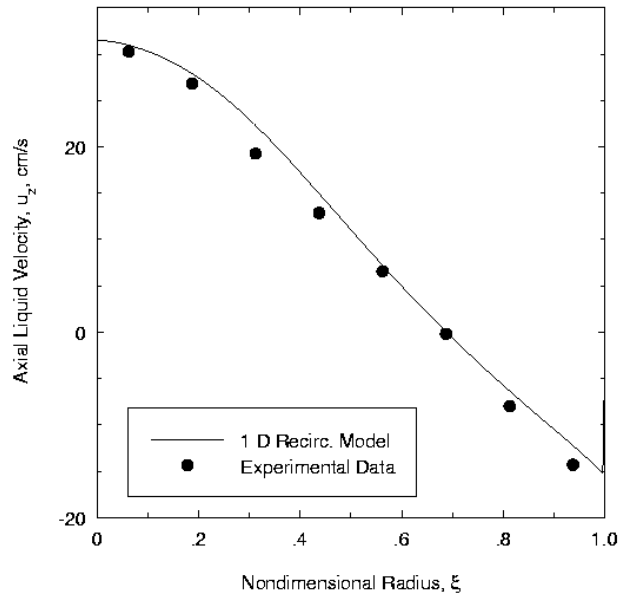


Figure 2.3 Time-Averaged, One-Dimensional Axial Liquid Velocity Profile: Column Diameter 19 cm, $U_g = 10$ cm/s

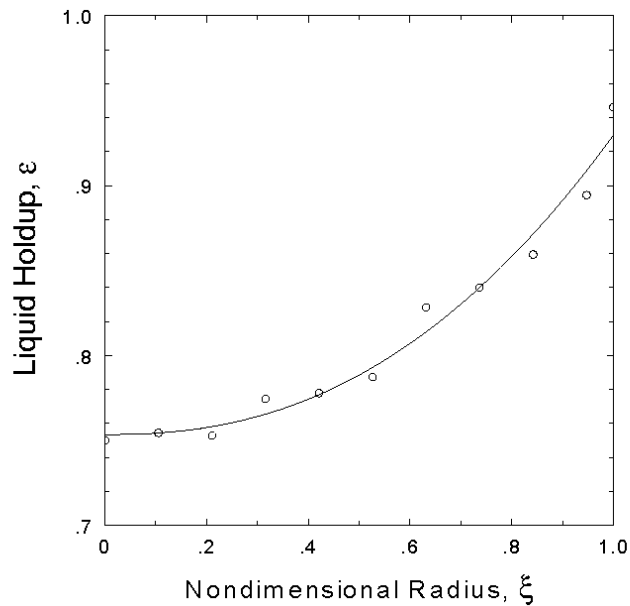


Figure 2.4 Time Averaged Liquid Holdup Profile: Column Diameter 19 cm, $U_g = 10$ cm/s

In Figure 2.3, the solid circles represent the axial liquid velocity axially averaged in the middle section of the column. The curve is the one-dimensional recirculation model prediction, using the input holdup profile from CT measurements (shown in Figure 2.4), along with a mixing length profile obtained from CARPT data. With these profiles for the liquid velocity and holdup, continuity is satisfied within 98%. The experimental data for the turbulent diffusivities, in Figure 2.5, are directly used as input to the model.

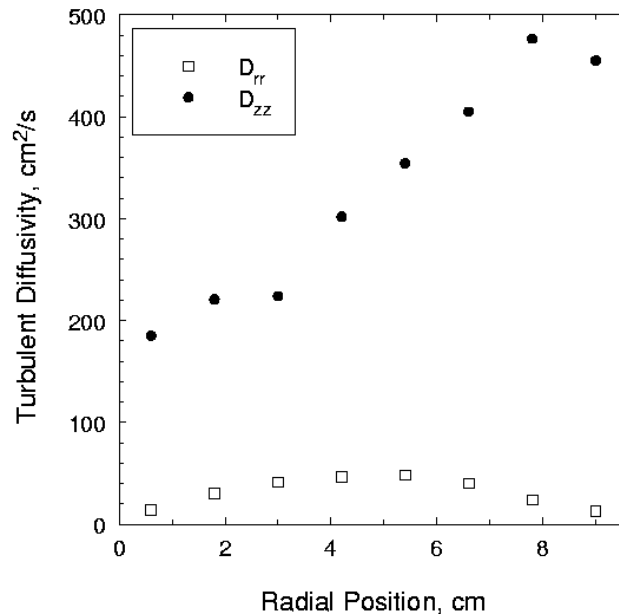


Figure 2.5 One Dimensional Turbulent Eddy Diffusivities: Column Diameter 19 cm, $U_g = 10$ cm/s

With the above parameters as input, the model (i.e., Equation 2.10) is solved to predict the overall tracer impulse response of the given system, shown in Figure 2.6. Here, $E(t)$ is evaluated as follows:

- i. The model (via equation 2.10) calculates $C(r, z=L, t)$.
- ii. The mixing cup concentration is calculated by Equation 2.14 a.
- iii. $E(t)$ is then calculated by Equation 2.14 b.

$$\bar{C}(z=L, t) = \frac{\int_0^R r \epsilon u_z C(r, z=L, t) dr}{\int_0^R r \epsilon u_z dr} \quad (2.14 a)$$

$$E(t) = \frac{\bar{C}(z=L, t)}{\int_0^\infty \bar{C} dt} \quad (2.14 b)$$

The comparison between the two-dimensional model prediction of the normalized exit mixing cup concentration and the experimental tracer response curve from Myers et al. (1986) (Figure 2.6) suggests that the model provides a good representation of the experimental data. Therefore, a fundamentally based model, with experimental data for the fluid dynamic parameters, is able to capture the overall mixing in the system as described by the tracer residence time distribution (RTD).

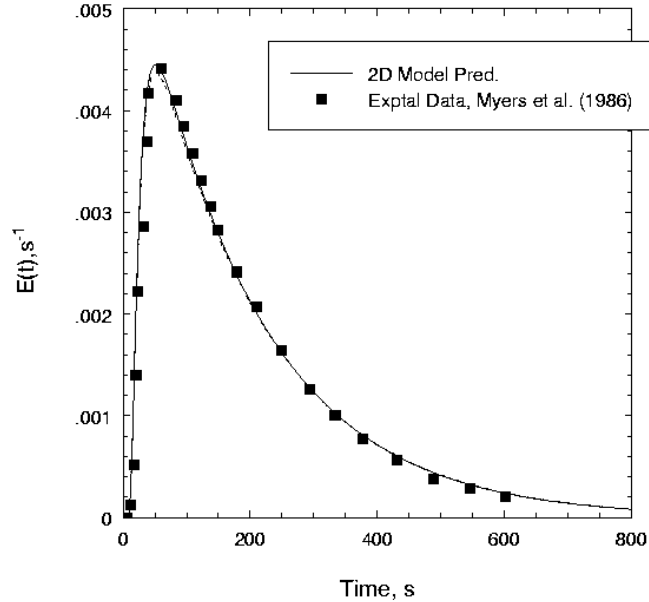


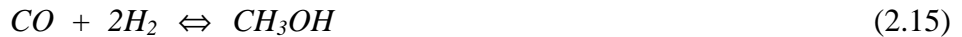
Figure 2.6: Comparison of Experimental Tracer Response with 2D Model Prediction (dashed line is for cell heights in end zones, equal to two column diameters while solid line is for heights of end zones equal to one column diameter).

2.4 Case II: Interpretation of the AFDU Tracer Data

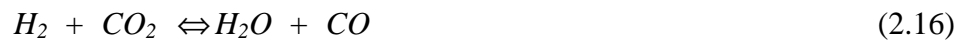
2.4.1 Experimental Details

The radioactive tracer experiments were conducted by Air Products and Chemicals, Inc. in DOE's LaPorte, Texas Alternate Fuels Development Unit (AFDU), which is a slurry bubble column reactor, to study the backmixing characteristics of the gas and liquid phase in this reactor during methanol synthesis. Powdered methanol catalyst (~45 wt % loading) suspended in an inert hydrocarbon oil forms the batch slurry phase. Synthesis gas is bubbled through a sparger placed at the bottom of the reactor. The gas disengages from the oil in the freeboard section of the reactor, and the unreacted feed gas is recycled back to the reactor.

The principal reaction for methanol synthesis is



At the process conditions used, the methanol formed is in the vapor phase. The feed gas to the reactor is synthesis gas, which is a mixture typically consisting of CO (30%), H_2 (60%), CO_2 (5%) and inerts (N_2). The composition of the feed gas may be varied by changing the feed ratio, depending upon process requirements. The presence of CO_2 is usually required, as it serves to initiate the reaction. A side reaction known to occur is the water gas shift reaction:



Based on the above reaction stoichiometry (Equations 2.15 and 2.16), there is a reduction in the volume of the gas due to reaction. The actual reduction depends on the feed rate, composition, and conversion. For the tracer runs studied, feeds with varying composition were used. The experimental conditions along with the feed compositions, observed conversions and changes in gas volumetric flow rate are reported in Table 2.1. The conversion of *CO* for the three runs studied ranges from 16% to 33%. An excess of *CO* results in lower conversion (Runs 14.6 and 14.7 compared to Run 14.8). Although *CO* conversion varies for the three cases, due to a corresponding change in feed composition, the effective overall change in the gas flow rate is about the same for all runs, around - 18%.

Table 2.1 Experimental Conditions (Temp : 250°C)

Run No.	P MPa	Avg. Gas Holdup	Inlet U_{g0} cm/s	Feed Compn. Mol %			Conv of <i>CO</i> to MeOH	Inlet Vol. Flow Rate SCFH	Change in Flow Rate %
				H_2	<i>CO</i>	CO_2			
14.6	5.2	0.39	25	35.4	50.8	12.7	15.9	143121	-17.1
14.7	5.2	0.33	14	35.0	50.9	12.7	17.5	81151	-19.2
14.8	3.6	0.38	36	60.2	24.0	10.3	33.0	141690	-17.7

2.4.2 Gas Holdup Measurements

Holdup measurements within the reactor were made using two techniques: 1. Differential Pressure (DP) measurements and 2. Nuclear Density Gauge (NDG) measurements. From the experiments conducted, there is no definite trend for the axial gas holdup at different velocities. In addition, discrepancies exist between the two techniques.

DP measurements rely on the assumption that liquid (slurry) velocities and shear stresses near the wall are small in comparison with the hydrostatic head. Thereby

$$\rho g = \frac{\Delta P}{\Delta z} \quad (2.17)$$

where

$$\rho = \rho_l \epsilon_l + \rho_g \epsilon_g \quad (2.18)$$

The subscripts 'l' and 'g' refer to the slurry and gas phase, respectively. Based on experimental evidence, the slurry density in the column is assumed to be uniform (ρ_l) and is calculated using the information on solids holdup ((catalyst weight/density) / dispersion volume) (Shollenberger 1995b). Therefore, from here on, the terms 'liquid' and 'slurry' are used interchangeably. The density of the gas phase is very small when compared with that of the slurry, and hence the second term in Equation 2.18 is usually ignored. Equation 2.18 in conjunction with Equation 2.17 can be used to calculate the average holdup between the two measurement sections (Figure 2.7). Assuming that there is no axial variation of holdup between the measurement sections, the volume average holdup calculated from DP measurements yields a cross-sectional mean holdup, $\bar{\epsilon}_g$:

$$\bar{\varepsilon}_g = 2 \int_0^1 \xi \varepsilon_g(\xi) d\xi \quad (2.19)$$

Nuclear Densitometry (NDG) is a noninvasive method in which a narrow beam of radiation (γ ray) emitted through the center of the column, with the source on one side (Figure 2.7), is detected using a detector on the opposite side. Such a single chordal measurement obtained across the centerline (i.e., diameter) of the column results in a chordal average, $\hat{\varepsilon}_g$, defined by

$$\hat{\varepsilon}_g = \int_0^1 \varepsilon_g(\xi) d\xi \quad (2.20)$$

which is not necessarily representative of the cross-sectional mean.

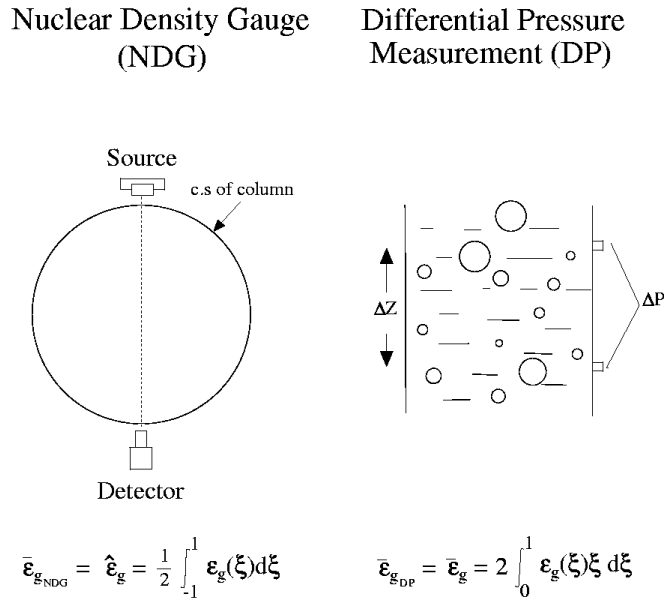


Figure 2.7 Schematic of DP and NDG Technique for the Measurement of the Average Gas Holdup

Therefore, there is a discrepancy between the average holdups measured by DP and NDG. Using Equation 2.11 for the radial gas holdup profile, the two averages $\bar{\varepsilon}_g$ and $\hat{\varepsilon}_g$ are found to be related by the following expression:

$$\frac{\hat{\varepsilon}_g}{\bar{\varepsilon}_g} = \frac{(m+2)(m+1-c)}{(m+1)(m-2c+2)} \quad (2.21)$$

Since experimental measurements of $\hat{\varepsilon}_g$ and $\bar{\varepsilon}_g$ are available from NDG and DP, the axial average of these values is used to extract the void fraction exponents m and c in Equation 2.11, given above, which then provide the description of the radial void fraction profile existing in the